Jewel Journal of Scientific Research (JJSR) 10(2): 213–222, 2025
©Federal University of Kashere-Nigeria (Print ISSN: 2384 – 6267, Online ISSN 2756-651X)
https://journals.fukashere.edu.ng/index.php/jjsr

Investigation of the Fluoroperovskite $LiBaF_3$, Examining the Optical, Elastic, Electronic and Structural Properties: DFT Study.

Olawale, E. O.[1], Adekoya, A. A.[2], Akinsola, S.I[1*] and Alabi, A. B.[1]
[1] Department of Physics, University of Ilorin, Nigeria.
[2] Department of Physics, Al-Hikmah University, Ilorin, Nigeria.
[*]**Corresponding Author**: akinsola.si@unilorin.edu.ng; +2348166602544

Abstract
The Structural, electronic, elastic and optical properties of the fluoroperovskite $LiBAF_3$ are obtained using the plane-wave pseudopotential implementation of the PWscf code method in the framework of density functional theory (DFT), with the local density approximation (LDA) and the generalized gradient approximation (GGA). The result shows LiBAF3 compound has a direct band gap with 6.7eV and 6.5eV using PBE-GGA and PBEsol-GGA respectively. It satisfies the Born's stability condition and thus implies the compound is stable. Refractive index, coefficient of extinction and dielectric function have all been computed. From the estimations, the material has a brittle feature. The values gotten are in close agreement with related works and further investigation can be done using other exchange correlation functional.

Keywords: Fluoroperovskites, Band Structure, Elastic properties, Structural properties
Received: 15th Sept, 2025 *Accepted:* 10th Nov, 2025 *Published Online:* 25th Dec, 2025

Introduction

There has been extensive attention given to Perovskite structure as a result of its remarkable properties like high thermoelectric power charge ordering, spin-dependent transport, colossal magneto-resistance and the chemistry of structural, magnetic, electronic and optical characteristics (Moskvin *et al.*, 2010, Weeks and Franz, 2010). Largely, they have a wide band gap which brands them a perfect material for optical lithography and production of vacuum ultraviolet lenses (Murtaza *et al*., 2013).

In the family of ternary compounds, Fluoroperovskites is a subgroup of perovskites. These materials are fluoride-based with a communal stoichiometry of ABF_3. 'A' and 'B' are cations. In the new perovskite material, 'A' cation is a mono or divalent element represented by an alkali or rare earth metals whereas 'B' cation is represented by Alkaline metals. These amazing material being referred to as Fluoroperovskites have recently received more thoughtfulness because of their possible usage as lens materials (Boyer and Edwardson, 1990; Lim and Jeong, 2005). Among the ternary compounds, $LiBaF_3$ single crystal is a candidate for vacuum-ultraviolet-transparent (VUV-transparent) material for lenses in optical lithography steppers, which finds good applications in the semiconductor industry sooner (Nishimatsu, *et al.*, 2002).

In this work, a well-thought-out study of the structural, electronic, elastic and optical properties of $LiBaF_3$ by using the plane-wave pseudopotential implementation of the PWscf code method in the framework of density functional theory (DFT) is reported. This is done with the local density approximation (LDA) and the generalized gradient approximation (GGA).

Computational Method

In this work, Density functional theory (Hohenberg and Kohn, 1964) is engaged to perform the calculations in union with the

method of plane-wave pseudopotential implementation of the PWscf method as implemented in the Quantum Espresso code. Also, the local density approximation (LDA) (Perdew and Wang, 1992), Perdew-Burke-Ernzerhof (PBE) and Perdew-Burke-Ernzerhof for solids (PBEsol) of the generalized gradient approximation (GGA) (Perdew, *et al.*, 1996) flavor are used to compute the exchange-correlation energy function. The tool used for modelling the interaction of electrons with ionic cores is the Ultrasoft pseudopotentials. The electronic wave functions and charge density were lengthened in a plane-wave basis sets up to kinetic energy cutoffs of 50 and 400 Ry, respectively. Brillouin-zone integration was performed using 7×7×7 Monkhorst-Pack k-point mesh. The above computational parameters were good enough to guarantee the accuracy of present purpose.

To determine the elastic nature, the elastic constants C_{ij} of $LiBaF_3$ compounds are estimated. Thermo_pw implemented in Quatum Espresso code was used to calculate the elastic properties. Basically, there are three main elastic constants named C_{11}, C_{12} and C_{44} for cubic crystals. The mechanical properties include bulk modulus *B*, voigt shear modulus *G*, Young's modulus *E*, Poisson's equation and Lame's coefficients (μ and λ).

From the elastic constants, notable elastic moduli for applications can be calculated:

$$B = \frac{1}{3}(C_{11} + 2C_{12}) \quad (1)$$

$$G = \frac{1}{5}(C_{11} - C_{12} + 3C_{44}) \quad (2)$$

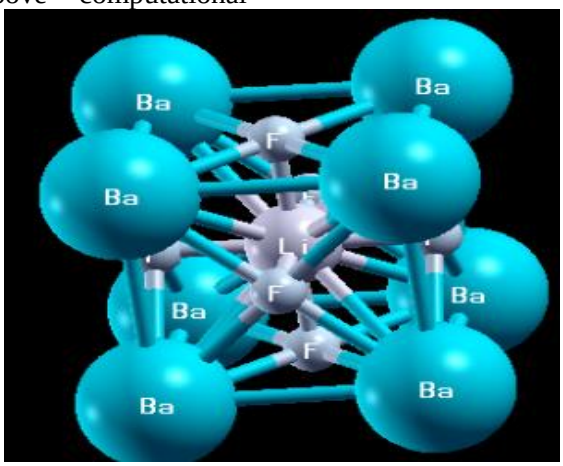

Figure 1. Crystal structure of $LibAF_3$

Results and Discussion

Structural properties

This section presents the structural properties of the system understudy. The optimized lattice parameters **(*a*)**, bulk modulus **(*B*)** and the pressure derivate of the bulk modulus **(*B'*)** is presented in Table 1. Table 1 shows there is large closeness between the calculated, prior reported and experimental value of the lattice parameter (*a*).

Table 1. Lattice constant (a), bulk modulus (B) and pressure derivative of bulk modulus (B') of $LiBaF_3$

Lattice constant $\mathbf{a}_\circ$(Å)	$\boldsymbol{B}_\circ$ (GPa)	$\boldsymbol{B'}_\circ$	Reference
4.038	226.8	6.86	This work [a]
4.045	271.9	4.61	This work [b]
3.969	313.5	4.96	This work [c]
3.994			(Ouenzerfi, *et al.*, 2004)[d]
3.934			(Ouenzerfi, *et al.*, 2004)[d]
3.996			(Boumriche, *et al.*, 1994)[e]

[a] LDA calculations; [b] GGA (PBE) calculations; [c] GGA (PBEsol) calculations; [d] Theoretical calculations; [e] Experiment

Elastic properties

$LiBaF_3$ has a cubic structure. Three elastic constants, C_{11}, C_{12}, C_{14} exist for the cubic structure of this compound. The elastic properties of the system are presented in this section. LDA and GGE (PBE and PBEsol) approximations were employed. The elastic constants and elastic moduli of the cubic unit cell has been calculated using the Voigt-Reuss-Hill approximation.

C44 exhibits resistance to shear deformation whereas C11 is linked to the unidirectional compression along the principal crystallographic directions. This indicates that the compound exhibits less resistance to pure deformation in comparison to their resistance to unidirectional compression (Mousa, *et al.*, 2017).

Elastic stability is the ability of a material to return to its original shape after the removal of compressive loads. For a cubic structure, the Born's stability condition is: $C_{11} - C_{12} > 0$; $C_{11} + 2C_{12} > 0$; $C_{44} > 0$. Our calculations fulfill these conditions. It thus implies the material is stable elastically in all approximations.

Table 2. Calculated values of elastic constants C_{ij} (in GPa), shear modulus *G* (in GPa), bulk modulus *B* (in GPa), Young's modulus *E* (in GPa), Poisson's ratio σ, Debye temperature (in *K*) and Pugh ratio.

	C_{11}	C_{12}	C_{44}	**B**	**E**	**G**	Σ	D.T	B/G
LDA	80.83	6.24	45.33	22.78	80.97	44.60	-0.092	401.17	0.51
PBE	117.89	42.50	42.80	78.76	117.87	47.13	0.2506	433.85	1.67
PBEsol	138.02	49.13	49.00	67.63	101.65	40.68	0.2495	396.72	1.67

For materials with ionic properties, it has a standard Poisson's ratio σ of 0.25 or higher and for materials with covalent bond, it has a value of 0.1 or lower. From the PBE and PBEsol calculations, it indicates the material has ionic properties. A central force material is a material that has its Poisson value within 0.25 and 0.5; otherwise, it is a non-central force material. The material is then a central force material. Pugh ratio indicates ductility or brittleness of a material. Pugh's index of ductility ratio has a critical value of 1.75. If B/G > 1.75, the material tends to ductility; otherwise, the material tends to brittleness. As shown above, B/G ratio is less than 1.75. It implies the material tends to be brittle. High value of Young's modulus *E* indicates a stiff material. The Debye temperature (Θ_D) is an important parameter calculated from elastic constant. Debye temperature has a close link with several physical properties, such as specific melting temperature. The sound velocities as calculated is presented in table III.

Table 3. Sound velocities

	V_P (m/s)	V_B (m/s)	V_G (m/s)
LDA	3981.87	2095.63	2932.19
PBE	5146.35	3838.15	2969.03
PBEsol	4918.37	3663.93	2841.57

There are no published data that discuss these properties for this compound to the best of our knowledge. Further studies will validate and test this outcome.

Optical Properties

Optoelectronic applications of a material can be understood by studying the optical property of the material. The dielectric function $\mathcal{E}(\omega)$, representing the linear response of the system to an external electromagnetic field with a small wave vector describes the optical properties of a matter. The dielectric function can be expressed as (Tell, 1956; Landau and Lifshitz, 1984; Kramers, 1956; Kronig, 1926)

$$\mathcal{E}(\omega) = \mathcal{E}_1(\omega) + \mathcal{E}_2(\omega) \quad (3)$$

$\mathcal{E}_1(\omega)$ is the real part of the dielectric function while $\mathcal{E}_2(\omega)$ is the imaginary part of the dielectric function. The imaginary elements of the dielectric function $\mathcal{E}_2(\omega)$ consist of the sum of all transitions from the valence bands to the conduction bands. The real part of the dielectric function $\mathcal{E}_1(\omega)$ can be extracted from the extracted from the imaginary part using the Kramers-Kroning relation (Mousa, 2014; Mousa, 2013). The dielectric function was calculated via the thermo_pw.x package.

Refractive index $n(\omega)$ and the Extinction coefficient $k(\omega)$ which are optical constants can be calculated in terms of the imaginary and real part of the complex dielectric function (Born and Huang, 1954; Tvergaard and Hutshinson, 1988; Haines, *et al.*, 2001).

$$n(\omega)=\sqrt{\frac{\sqrt{\varepsilon_1^2(\omega)+\varepsilon_2^2(\omega)}+\varepsilon_1(\omega)}{2}} \quad (4)$$

$$k(\omega)=\sqrt{\frac{\sqrt{\varepsilon_1^2(\omega)+\varepsilon_2^2(\omega)}-\varepsilon_1(\omega)}{2}} \quad (5)$$

Coefficient of absorption $I(\omega)$ and reflectivity $R(\omega)$ can also be calculated along the xx-direction.

Figures 2 and 3 show the real and imaginary part of the dielectric constant respectively.

$\mathcal{E}_1$, real part of the dielectric constant exhibit peaks 5.1 at 8.8eV, 5.4 at 9.8eV and 2.6 at 20eV while the imaginary part of the dielectric constant, $\mathcal{E}_2$ exhibit peaks 4.1 at 9eV, 4.4 at 10ev, 3.6 at 12eV and 3 at 20eV. This typifies close proximity with related materials (Korba, *et al.*, 2009). Electronic transitions between the valence and conduction band accounts for the threshold energy. The main peaks for $\mathcal{E}_1$ and $\mathcal{E}_2$ exist at 9.8eV and 10eV for this material. From observation, there is a steep decrease between 9.8eV and 10.5eV for the real part of the dielectric function and a steep decrease between 10ev and 11eV in the imaginary part of the dielectric function.

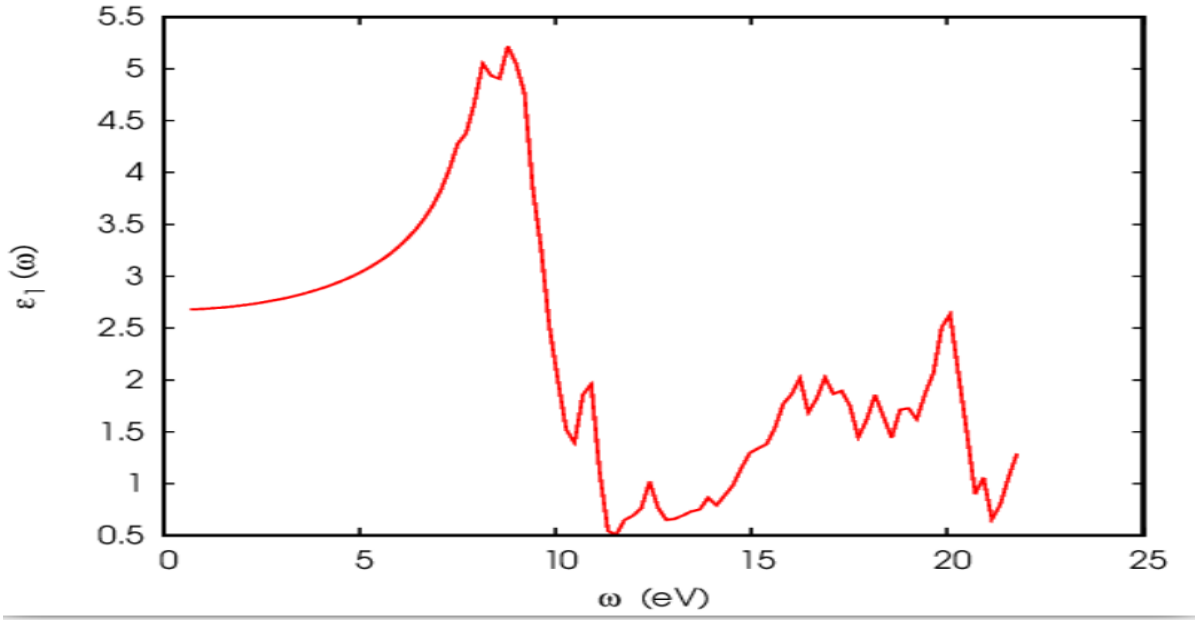

Figure 2. Real part of the dielectric function

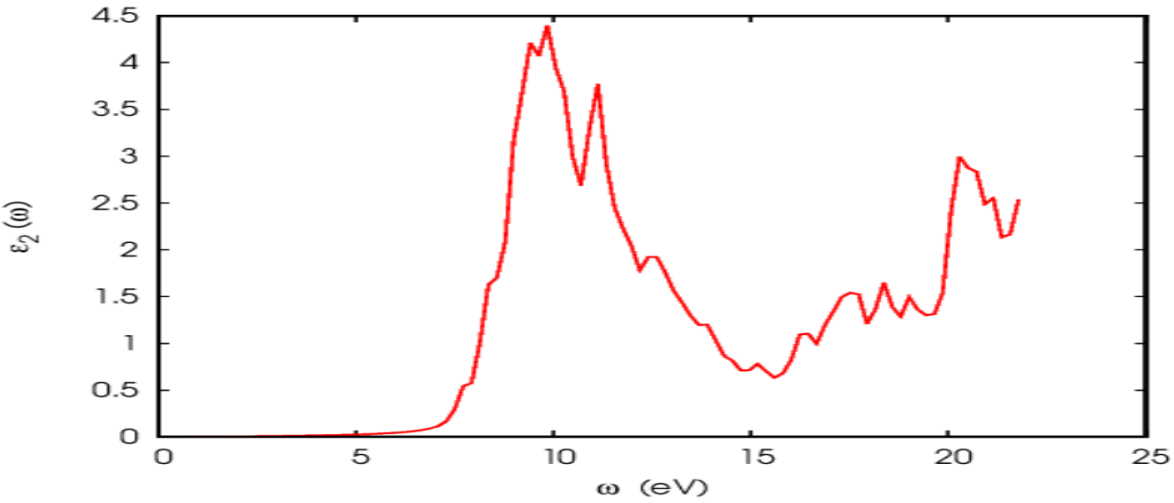

Figure 3. Imaginary part of the dielectric function

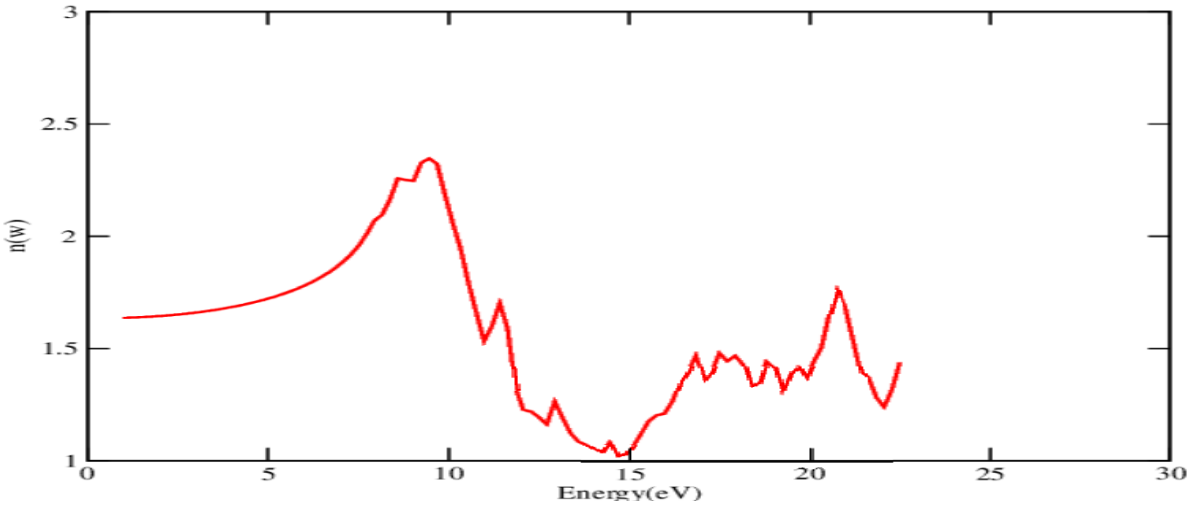

Figure 4. Refractive index n(ω)

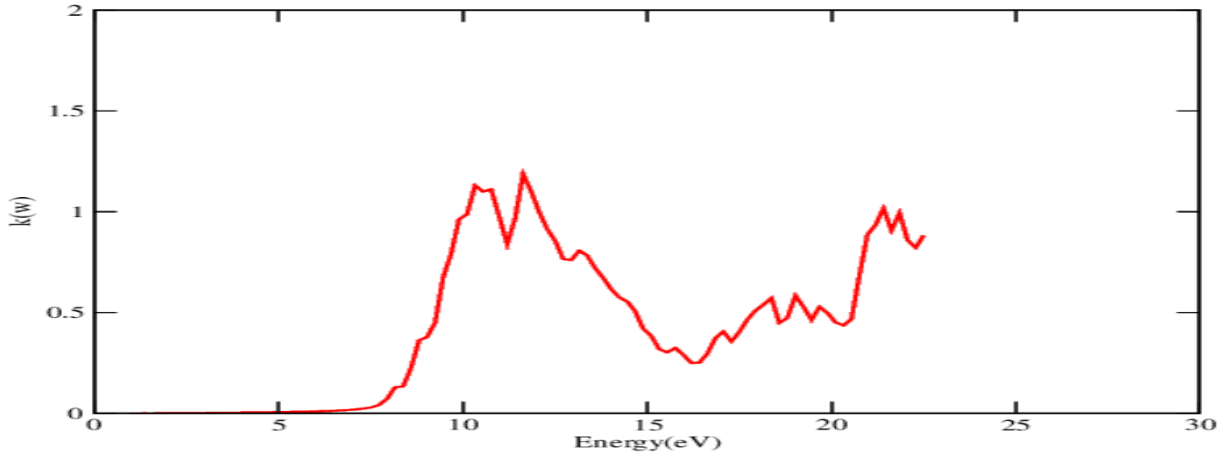

Figure 5. Extinction coefficient k(ω)

The extinction coefficient and refractive index have been calculated as shown above. It is observed that there is resonance in the low energy region in this compound. The obtained refractive index spectra indicate that the refractive index is majorly only up to 11 eV. Refractive index drops significantly beyond this energy.

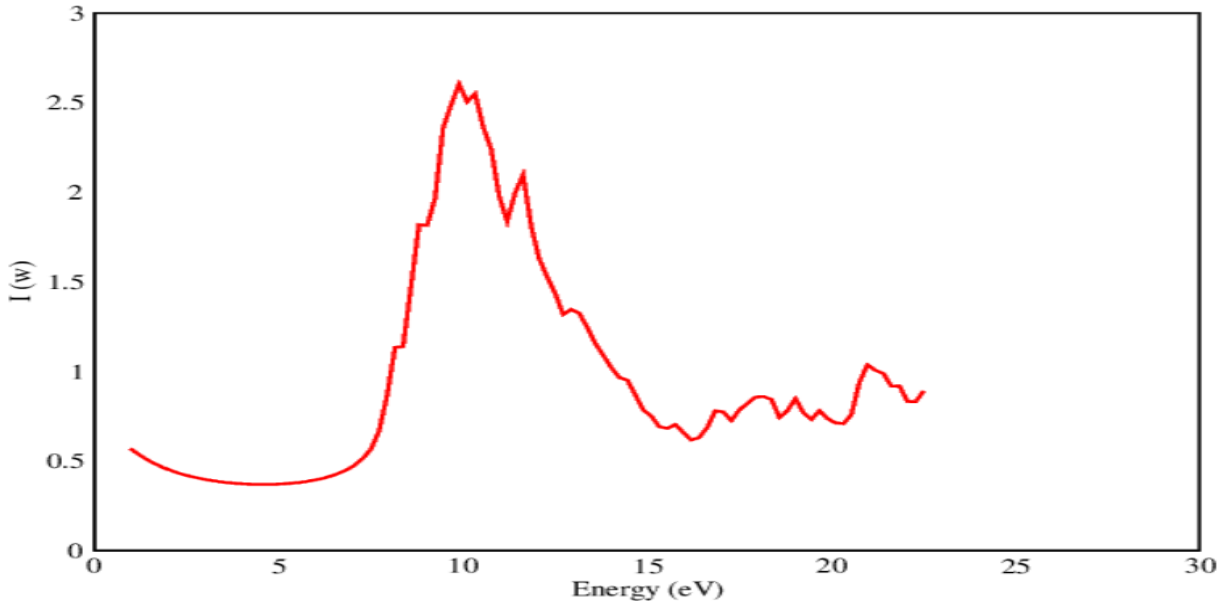

Figure 6. Calculated absorption coefficient I(ω) of the dielectric function E(ω) for $LiBaF_3$

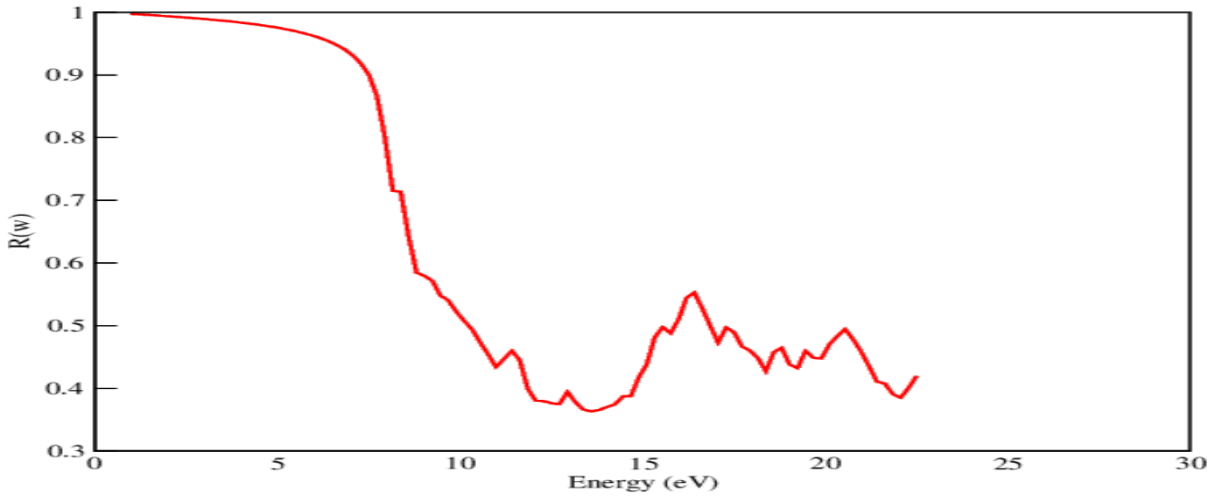

Figure 7. Calculated reflectivity R(ω) of the dielectric function E(ω) for $LiBaF_3$

Figures 6 and 7 shows the calculated absorption coefficient and reflectivity spectra of $LiBaF_3$. In the reflectivity spectrum, it is observed that there's high reflectivity at low energies. This can be an indication that the material is highly transparent in the infrared, visible and low-frequency ultraviolet region of the energy spectrum. It then be suggested that this material will be an efficient lens material and possibly applicable for transparent coating.

Electronic Properties

This section reports the band structure and partial density of state of $LiBaF_3$, GGA flavor of the exchange correlation potentials namely Perdew-Burke-Ernzerhof (PBE) and Perdew-Burke-Ernzerhof for solids (PBEsol) were used. The computed electron energy band

structure calculations along some important symmetry directions are shown in Figures 8 - 9. The material has a direct band gap and it is a wide-gap perovskite-like-fluorides

Table 4: Energy gap values

PBE	*PBEsol*	Reference
6.7eV	6.5Ev	This work [a]
6.66eV		(Korba, *et al.*, 2009)[b]
6.513eV		(Besnalah, *et al.*, 2003)[b]
9.8eV		(Sarukura, *et al.*, 2007)[c]

[a] PBE and PBEsol calculations [b] Theoretical calculations [c] Experiment

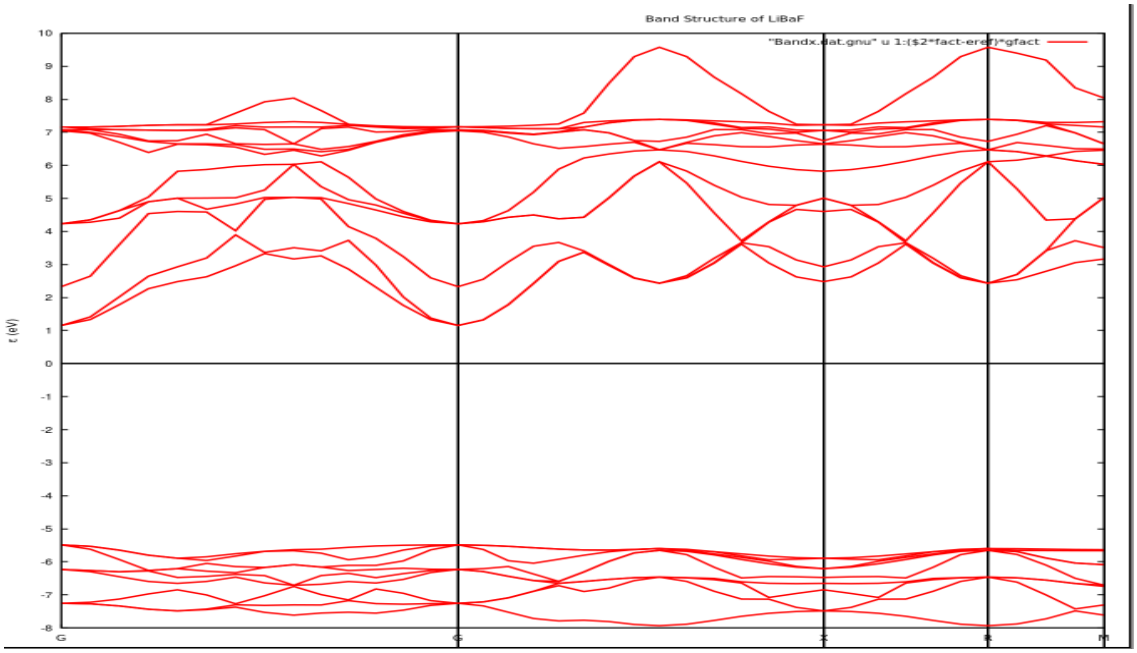

Figure 8. PBEsol flavor energy band plot

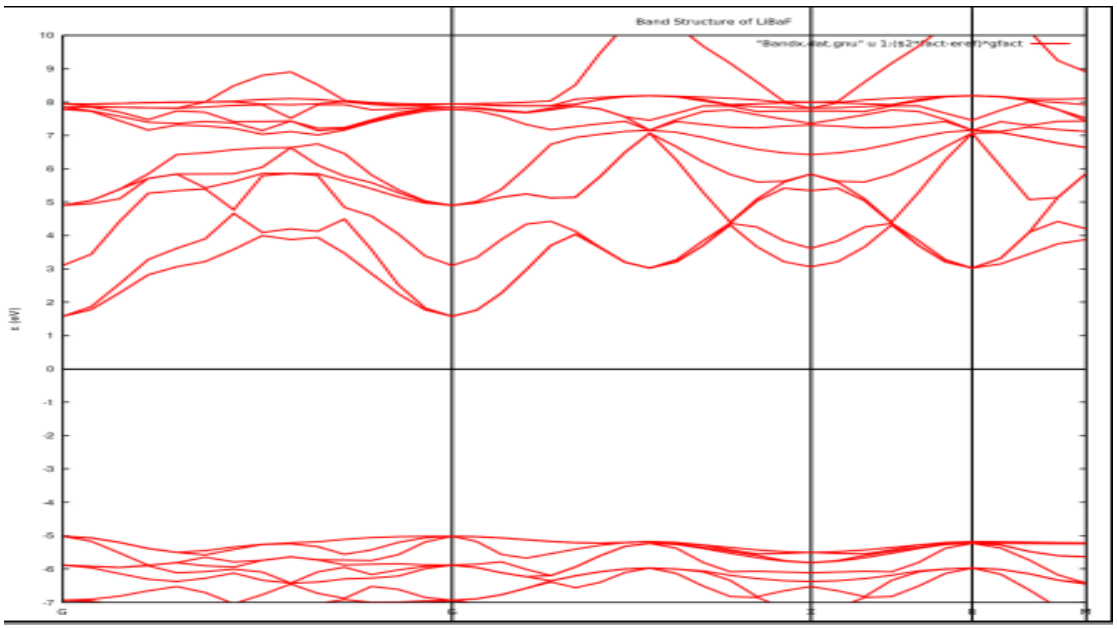

Figure 9. PBE flavor energy band plot

It is generally known that GGA often underestimate the energy gap (Charifi., 2005; Hassan, *et al.,* 2004). This is because it has single form that is not flexible sufficiently for accuracy in producing exchange-correlation energy and its charge derivative. The values gotten are in close agreement with available results. Figure 10 and figure 11 shows the calculated PDOS of BA, Li, and F atoms.

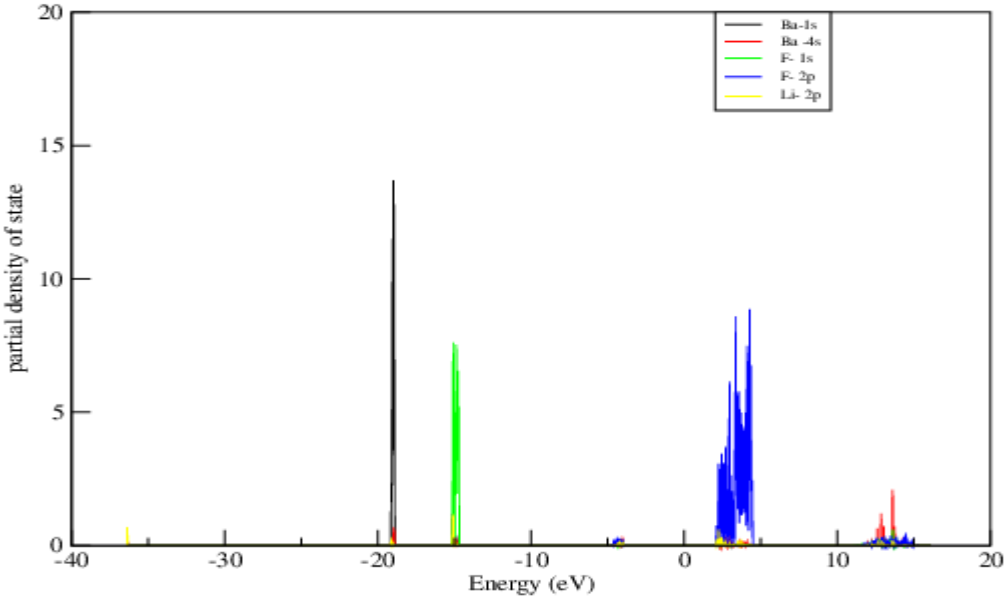

Figure 10. pdos plot of $LiBaF_3$ [PBEsol]

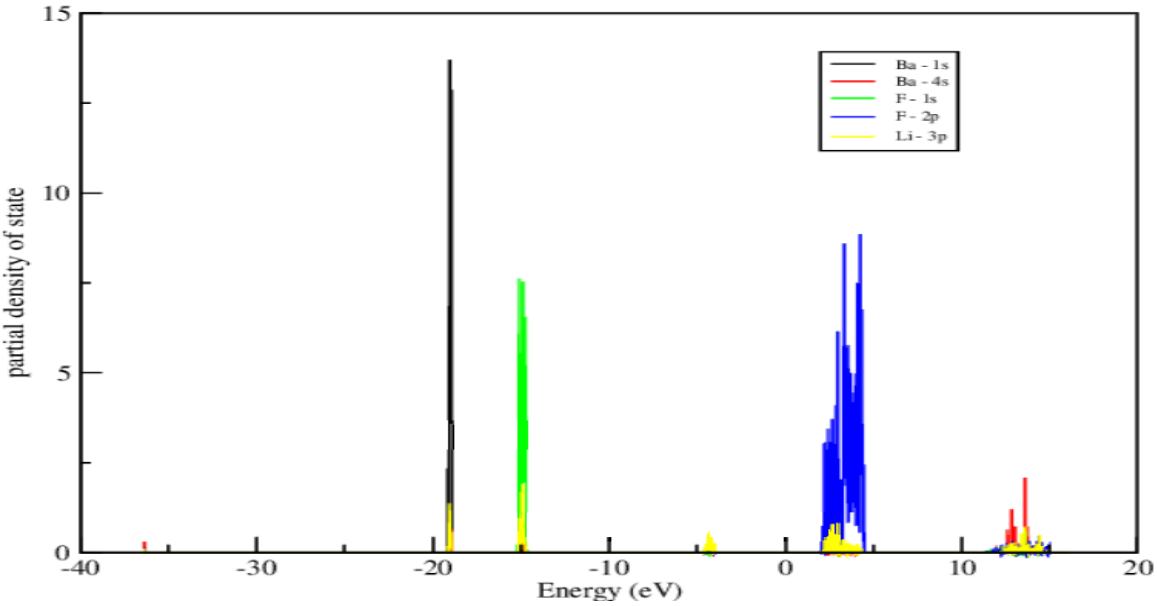

Figure 11. pdos plot of $LiBaF_3$ [PBE]

Data Availability Statement:
Data cannot be shared openly but are available on request from authors:
Data sets generated during the current study are available from the corresponding author on reasonable request.

Conclusion

The structural, electronic, elastic and optical properties of $LiBAF_3$ were studied using the method of plane-wave pseudopotential implementation of the PWscf method as implemented in the Quantum Espresso code. This is based on density functional theory using the LDA and GGA flavor of the exchange correlation. The calculated electronic structure and energy band structure shows a direct band gap. Similarly, the real and imaginary part of the dielectric constant, refractive index, extinction coefficient, absorption coefficient and refractivity have been calculated. Elastic properties were calculated as well. From calculation, the material has a tendency to be brittle. The values gotten are in close agreement with related works and further investigation can be done using other exchange correlation functional.

References

Besnalah, A., K. Shimamura, T. Fujita, H. Sato, M. and Nikl, T. F. (2003). Growth and characterization of $BaLiF_3$ single crystal as a new optical material in the VUV region. *Journal of Alloys and Compounds.* 348 (1): 258-262. https://doi.org/10.1016/S0925-8388(02)00827-7

Born, M. and K. Huang. (1954). Dynamical Theory of Crystal Lattices. 1st edition. *Clarendon Press, Oxford.*Pp. 431.

Boumriche, A., Gesland, J.Y., Bulou, A. and Rousseau, M. (1994). Structure and dynamics of the inverted perovskite $BaLiF_3$. *Solid State Commununication.* 91 (2): 125-128. https://doi.org/10.1016/0038-1098(94)90268-2

Boyer, L.L and Edwardson, P.J. (1990). Perovskite to antiperovskite in abf_3 compounds. *Ferroelectrics.* 104(1): 417-422. https://doi.org/10.1080/00150199008223849

Charifi, Z., H. Baaziz, F. El Haj Hassan and Bouarissa, N. (2005). High pressure study of structural and electronic properties of calcium chalcogenides. *Journal of Physics: Condensed Matter.* 17(26): 4083. **doi:**10.1088/0953-8984/17/26/008

Haines, J., Leger, J. M. and Bocquillon, G. (2001). Synthesis and Design of Superhard Materials. *Annual Review of Materials Research*. 31: 1-23. https://doi.org/10.1146/annurev.matsci.31.1.1

Hassan, F.E.H., H. Akbarzadeh, S.J. Hashemifar, A. Mokhtari. (2004). Structural and electronic properties of matlockite MFX (M=Sr, Ba, Pb; X=Cl, Br, I) compounds. *Journal of Physics and Chemistry of Solids.* 65 (11):1871-1878. https://doi.org/10.1016/j.jpcs.2004.07.002

Hohenberg, P. and W. Kohn. (1964) Inhomogeneous Electron Gas. *Physical Review B.* 136: 864-871. http://dx.doi.org/10.1103/PhysRev.136.B864

Korba, S. A, H. Meradji, S. Ghemid, B. Bouhafs. (2009). First principles calculations of structural, electronic and optical properties of $BaLiF_3$. *Computational Material Science*. 44 (4):1265-1271. https://doi.org/10.1016/j.commatsci.2008.08.012

Kramers, H.A. (1956). Collected Science Papers. North Holland, Amsterdam.178:337–338. doi:10.1038/178337b0

Kronig, R.D.L. (1926). On the Theory of Dispersion of X-Rays. *Journal of Optical Society of America.* 12: 547-556. http://dx.doi.org/10.1364/JOSA.12.000547

Landau, L.D. and E.M. Lifshitz. (1984). Electrodynamics in Continuous Media. *Pergamon Press, England.* https://doi.org/10.1016/B978-0-08-030275-1.50007-2

Lim, A.R. and S.Y. Jeong, (2005). A study of the NMR relaxation mechanisms of $ABCl_3$ (*A*=Rb, Cs, *B*=Cd, Mn) single crystals with the electric quadrupole and the electric magnetic types. *Journal of Solid State Chemistry*. 178 (10): 3095-3100. https://doi.org/10.1016/j.jssc.2005.07.024

Moskvin, A.S., A.A. Makhnev, L.V. Nomerovannaya, N.N. Loshkareva, and A.M. Balbashov. (2010). Interplay of p-d and d-d charge transfer transitions in rare-earth perovskite Manganites. *Physical Review B, Condensed matter* 82(3): 1-20.

https://doi.org/10.1103/PhysRevB.82.035106

Mousa, A.A. (2014). First-principles study of structural, electronic and optical properties of the $KCaX_3$ (X = F and Cl) compounds. *International Journal of Modern Physics B*. 28(21): 1-15. doi: 10.1142/S0217979214501392

Mousa, A.A, J.M. Khalifeh, N.T. Mahmoud, and H.K. Juwhari. (2013). First Principles Study of Structural, Electronic and Optical Properties of the Fluoroperovskite $RbCaF_3$ Crystal. *American Journal of Condensed Matter Physics.* 3(5):151-162. https://doi.org/10.5923/j.ajcmp.20130305.06

Mousa, A.A., M.S. Abu-Jafar, Diana Dahliah, R.M. Shaltaf and J.M. Khalifeh. (2017). Investigation of the Perovskite $KSrX_3$ (X = Cl and F) Compounds, Examining the Optical, Elastic, Electronic and Structural Properties: FP-LAPW Study. *Journal Electronics Materials*. 47: 641-650. https://doi.org/10.1007/s11664-017-5817-x

Murtaza, G., I. Ahmad, and A. Afaq, (2013) Investigation of optoelectronic properties of cubic perovskite $LaGaO_3$. *Solid State Sciences*. 16: 152-157. https://www.sciencedirect.com/journal/solid-state-sciences/issues

Nishimatsu, T., N. Terakubo, H. Mizuseki, Y. Kawazoe, D.A. Pawlak, K. Shimamuri and T. Fukuda. (2002). Band Structures of Perovskite-Like Fluorides for Vacuum-Ultraviolet-Transparent Lens Materials. *Japanese Journal of Applied Physics.* 41(4): 365. **doi:** 10.1143/JJAP.41.L365

Ouenzerfi, R. E, S. Ono, A. Quema, M. Goto, N. Sarukura, T. Nishimatsu, N. Terakubo, H. Mizuseki, Y. Kawazoe, A. Yoshikawa and T. Fukuda. (2004). Design Proposal of Light Emitting Diode in Vacuum Ultraviolet Based on Perovskite-Like Fluoride Crystals. *Japanese Journal of Applied Physics.* 43 (9): L1140-L1143. http://iopscience.iop.org/1347-4065/43/9A/L1140

Ouenzerfi, R.E, S. Ono, A. Quema, M. Goto, M. Sakai, N. Sarukura, T. Nishimatsu, N. Terakubo, H. Mizuseki, Y. Kawazoe, H. Sato, D. Ehrentraut, A. Yoshikawa and T. Fukuda. (2004). Design of wide-gap fluoride heterostructures for deep ultraviolet optical devices. *Journal of Applied Physics.* 96(12):7655-7659. repo.lib.nitech.ac.jp/handle/123456789/4375

Perdew, J.P. and Y. Wang. (1992). Accurate and simple analytic representation of the electron-gas correlation energy. *Physical Review B.* 45:13244-13249. http://dx.doi.org/10.1103/PhysRevB.45.13244

Perdew, J.P., S. Burke, and M. Ernzerhof. (1996). Generalized Gradient Approximation Made Simple. *Physical Review Letter.* 77: 3865-3868. http://dx.doi.org/10.1103/PhysRevLett.77.3865

Sarukura, N., H. Murakami, E. Estacio, S. Ono, R.E. Ouenzerfi, M. Cadatal, T. Nishimatsu, N. Terakubo, H. Mizuseki, Y. Kawazoe, A. Yoshikawa and T. Fukuda. (2007). Proposed design principle of fluoride-based materials for deep ultraviolet light emitting devices.*Optical Materials.* 30 (1):15-17. https://doi.org/10.1016/j.optmat.2006.11.031

Tell, J.S. (1956). Causality and the Dispersion Relation: Logical Foundations. *Physical Review.* 104:1760. https://doi.org/10.1103/PhysRev.104.1760

Tvergaard, V and J.W. Hutshinson. (1988). Microcracking in Ceramics Induced by Thermal Expansion or Elastic Anisotropy. *Journal of the American Ceramic Society.* 71(3):157-166. https://doi.org/10.1111/j.1151-2916.1988.tb05022.x

Weeks, C. and M. Franz. (2010). Topological insulators on the Lieb and perovskite lattices. *Physical Review B, Condensed matter.* 82(8):085310. https://doi.org/10.1103/PhysRevB.82.085310